ECOSYSTEMS

No Signs of Long-term Greening Trend in Western Mongolian Grasslands

Markus Hauck,[1]* Michael Klinge,[2] Stefan Erasmi,[3] and Choimaa Dulamsuren[1]

[1]*Applied Vegetation Ecology, Faculty of Environment and Natural Resources, University of Freiburg, Tennenbacher Str. 4, 79106 Freiburg, Germany;* [2]*Physical Geography, Institute of Geography, University of Göttingen, Goldschmidtstraße 5, 37077 Göttingen, Germany;* [3]*Thünen Institute of Farm Economics, Bundesallee 63, 38116 Braunschweig, Germany*

ABSTRACT

Trends for increased vegetation greenness based on satellite-derived data have been repeatedly published for the temperate grassland biome (including forest steppes) of eastern Inner Asia since 1982. Although this greening trend has been attenuated or partially reversed by drought in the early twenty-first century, linear increases in the Normalized Difference Vegetation Index (NDVI) or other parameters of vegetation greenness are nevertheless evident when the period since 1982 is regarded. However, the question arises whether these trends are part of a long-term trend driven by climate change, as simultaneously forests in the region show widespread drought-induced growth reductions and mortality outbreaks. Therefore, we hypothesized that the post-1982 greening trend was neither part of a long-term trend nor unprecedented. To test this hypothesis, we analyzed monthly maximum NDVI data from AVHRR time series and correlated these data with standardized tree-ring data of *Larix sibirica* from two regions of western Mongolia. We used linear regression to model the NDVI from tree-ring anomalies and to reconstruct the NDVI since 1940. These reconstructions show that the availability of satellite-based NDVI data coincidentally began during a dry period of low vegetation greenness in the early 1980s and was followed by a wet phase in the 1990s, producing the linear greening trend. No positive long-term trend in the reconstructed NDVI was observed from 1940 to 2010. This result rules out a recent climate change-driven greening trend for the grasslands and forest steppes of western Mongolia and calls into question its existence for all of eastern Inner Asia.

Key words: climate change; productivity; remote sensing; NDVI; tree-ring analysis; steppe; Siberian larch (*Larix sibirica*).

INTRODUCTION

Biome-wide shifts in the productivity of the vegetation have been observed in the recent past, which were attributed to global climate change as well as fertilization effects of rising atmospheric CO_2 and reactive nitrogen levels (Zhu and others 2016). Large-scale monitoring of vegetation productivity is typically performed using the Normalized Differ-

ence Vegetation Index (NDVI) or related vegetation indices (for example, the fraction of photosynthetically active radiation absorbed by the vegetation, FPAR) derived from satellite-based remote sensing data to provide an estimate of vegetation greenness. 'Greenness' largely reflects the density of chlorophyll and thus encompasses the leaf area index and vegetation vigor in a bulk parameter (Anyamba and Tucker 2012). The leaf area is closely related to the photosynthetic capacity and both parameters are strong determinants of biomass production in any terrestrial ecosystem (Kruger and Volin 2006). Therefore, the NDVI and other remote sensing parameters can be used to predict net primary production (Ruimy and others 1994; Schloss and others 1999; Liu and others 2021).

The Arctic tundra shows a consistent greening trend due to rapid climate warming at high latitudes (Goetz and others 2005). Arctic greening is only sporadically interrupted by reverse trends for browning (Lara and others 2018), which can be triggered by frost damage resulting from reduced winter snowpack, insect and fungal infestations, or fire (Bjerke and others 2017). Boreal forests, originally expected to benefit from climate warming throughout their range (Jarvis and Linder 2000), exhibit a divergent response with increased productivity at sites well supplied with water (for example, most alpine and polar forest lines) and decreased productivity if water becomes limiting, which is particularly relevant under continental climates and at the southern distribution limit of the boreal forest biome (Beck and others 2011; Tei and others 2017; Babst and others 2019; Dulamsuren and Hauck 2021). Buermann and others (2014) demonstrated that more and more boreal forests have switched from temperature limitation to drought limitation as climate warming progresses. Temperate forests in Europe, Asia, and North America have also experienced increases in productivity, which have been attributed to climate change, eutrophication, CO_2 fertilization, and altered land-use practices (Gedalof and Berg 2010; McMahon and others 2010; Pretzsch and others 2014).

Trends of increasing productivity have also been published for the steppe biome, which represents temperate, winter-cold grasslands primarily in the centers of the Eurasian and the North American continents. Prevalent greening trends across the steppes of Eurasia and North America were detected by Nemani and others (2003) between 1982 and 1999 and de Jong and others (2012) between 1982 and 2008 using FPAR or NDVI data, respectively. Hicke and others (2002) published an NDVI-derived greening trend for the North American steppe region from 1982 to 1998. For the Mongolian–Chinese steppe region of Inner Asia, several authors detected greening trends from, respectively, 1982 to 1999 (Zhou and others 2001; Piao and others 2006), 1982 to 2008 (Guay and others 2014), 1982 to 2015 (Meng and others 2019; Miao and others 2021), and 1982–2016 (Zhang and others 2021) based on NDVI data. These repeatedly demonstrated increases in the NDVI went along with similar increases in the grasslands and semi-deserts of Xinjiang (1982–2003; Zhao and others 2011) and the grasslands of the Tibetan Plateau (1982–2012; Wang and others 2016).

Despite this general greening trend for Inner Asia's grasslands, there are spatial and seasonal differences in the variability of vegetation greenness. Greening trends prevail in eastern Kazakhstan, in the Mongolian Altai of western Mongolia, in the northernmost parts of Mongolia (for example, in the Lake Khovsgol region) as well as in the eastern Mongolian grasslands (Poulter and others 2013; Miao and others 2021). In the forest steppes of the Khangai and Khentei Mountains of western and central Mongolia, areas of increasing and decreasing vegetation greenness alternate. In Inner Mongolia, greening trends are noted mainly for true steppes and forest steppes, but not for desert steppe (Piao and others 2003, 2006, 2015; Guo and others 2014; Miao and others 2021). Although springtime (March to May) vegetation greenness has increased throughout the steppe and forest-steppe region of Mongolia, summer (June to August) greening was mainly restricted to the Mongolian Altai, Lake Khovsgol, and parts of eastern Mongolia (1982–2010; Poulter and others 2013). Furthermore, the greening trends for Mongolia and eastern Kazakhstan have weakened in the twenty-first century, as shown by comparing NDVI trends from 1982 to 2009, 1990 to 2009, and 2000 to 2009 (Mohammat and others 2013). This weakening is attributable to an increased influence of drought on vegetation greenness, which counteracts positive effects of temperature and also affects other parts of the temperate zone outside Inner Asia (Piao and others 2011, 2014).

The repeated detection of multi-decadal trends for increased vegetation greenness in Mongolia and surrounding parts of Inner Asia contrasts with numerous reports from tree-ring studies evidencing prevalent declines in annual stem increment and even the widespread occurrence of drought-induced tree mortality (Dulamsuren and others 2010a, 2010b, 2013; Liu and others 2013; Khansaritoreh and others 2017a). Tree-ring width

in Mongolia's boreal forests has been shown to correlate with the maximum growing season NDVI of forested land (Erasmi and others 2021), corroborating that radial stem increment reflects overall forest productivity. The recent declines in the radial annual stem increment of trees are linked with increased summer drought as the result of climate warming at constant or reduced precipitation (Davi and others 2006, 2010; Dulamsuren and others 2011, 2013). Only in a minority of cases, especially at alpine tree lines (D'Arrigo and others 2001; Dulamsuren and others 2014), forests in Mongolia benefit from increased temperatures, provided that low temperatures limit productivity more than moisture. The prevailing trends for productivity declines at the southern edge of the boreal forest in Mongolia and surrounding regions of Inner Asia are part of a global trend for climate change-induced reductions in the productivity of boreal forests under continental climate (Buermann and others 2014; Babst and others 2019). The recent trend for a hotter and drier climate causing this widespread growth declines in Mongolia was unprecedented for at least 260 years (Zhang and others 2020).

Given that forests and grasslands intermingle in the forest-steppe ecotone between the boreal forest and the Central Asian steppe biome, the question is to reconcile the conflicting evidence of predominantly declining forest productivity inferred from tree-ring data and increasing vegetation greenness (including grasslands and forests) from remote sensing data. Theoretically, productivity trends in forests and grasslands could diverge due to differences in tree and grass ecophysiology or different site conditions in forested and non-forested areas (Brehaut and Danby 2018). However, published work linking vegetation greenness in Inner Asian steppes and to tree-ring data does not suggest that this is a likely explanation. While Erasmi and others (2021) established a relationship between standardized tree-ring data and the maximum growing season NDVI in the *Larix sibirica*-dominated forest steppe of western Mongolia, Liang and others (2006) found a similar relationship between tree-ring indices of *Pinus tabulaeformis* and *Picea meyeri* and mean growing season NDVI in the forest steppe of Inner Mongolia. Poulter and others (2013) established a positive correlation between the tree-ring anomalies from various sites across Mongolia and FPAR anomalies, however, by averaging data from sites that partially contrasted in climate and climate–growth relationships. Liang and others (2006) did not use their data for a direct reconstruction of the NDVI, but inferred from

variations in their tree-ring chronology, which started in 1850, that the increase in the NDVI observed from 1982 to 2001 was not unprecedented. Rather, it represented an episode during moisture-driven decadal oscillations in productivity with a return interval of 17–20 years, suggesting the absence of a unique, climate change-driven greening trend since the 1980s.

Combined with the evidence indicating widespread reductions in forest productivity, the results of Liang and others (2006) suggest that the significance of the greening trend since the 1980s, which has been repeatedly publicized from the steppes of Inner Asia, should be reassessed. Even though the existence of this trend is undisputed, we hypothesize that it does not reflect a long-term trend, but results from the coincidence that just by chance the observation period, for which satellite-based NDVI data are available, happened to begin in 1982. Verification of this hypothesis would imply that, unlike the greening trends observed in the Arctic tundra or at the northern edge of the boreal forest, the greening trend of the Inner Asian steppes is probably unrelated or only weakly related to climate change. Tree-ring chronologies from eastern Kazakhstan (Dulamsuren and others 2013), the Mongolian Altai (Dulamsuren and others 2014; Unkelbach and others 2021), the Khangai Mountains (Dulamsuren and others 2010a; Khansaritoreh and others 2017a, 2017b), and to some extent the Khentei Mountains (Dulamsuren and others 2010a) reveal negative relative growth extremes right in the early 1980s around 1980–1982.

Specifically, we tested our hypothesis using tree-ring and NDVI data from the Mongolian Altai and the western Khangai Mountains in western Mongolia. Although Poulter and others (2013) found a greening trend in both spring and summer for the Mongolian Altai, such trend was restricted to spring in the western Khangai. These different observations were due to a stronger drought limitation of the vegetation in the Khangai Mountains (Poulter and others 2013; Khansaritoreh and others 2017a, 2017b; Dulamsuren and Hauck 2021) than in the higher Mongolian Altai, where the growth of *L. sibirica* is primarily limited by low temperatures (Dulamsuren and others 2014). Based on Erasmi and others (2021), where we showed that modeling the maximum growing season NDVI with tree-ring data from *L. sibirica* forests is feasible, we aimed to reconstruct the NDVI for several decades prior to satellite-based NDVI records. Using these reconstructed values, we wanted to test the hypothesis that there has been no positive long-term trend for vegetation greenness since the mid-twentieth

century, whereas both calculated and modeled NDVI values have shown an upward trend since 1982. In addition, because Poulter and others (2013) found no greening during summer in the Khangai Mountains, we tested the hypothesis that these contrasting trends for monthly maximum NDVI values in summer for the two study areas are visible in the modeled data. With this case study from two climatically contrasting environments of western Mongolia, we aimed to draw a general conclusion as to whether or not a climate change-driven unprecedented long-term greening trend for the steppe grasslands of Inner Asia is likely.

MATERIALS AND METHODS

Study Area

The study was conducted in the two major forest-steppe regions of western Mongolia, that is, the Mongolian Altai and the western Khangai Mountains (Figure 1). The Mongolian forest steppe is composed of landscape units with varying proportions of grasslands and forested areas depending on topography and land-use history (Khansaritoreh and others 2017a; Erasmi and others 2021). Because we aimed at modeling vegetation greenness

in grassland-dominated areas from tree-ring data, we combined remote sensing data and dendrochronological data that were sampled from different subunits of our two study regions (Figure 1). Whereas the tree-ring data were taken from forest-dominated parts of the study regions, the remote sensing data were sampled from landscape units with high share of steppe grassland. Areas used for remote sensing analysis were thus located 25 km NNW of the forests used for tree-ring sampling in the Mongolian Altai and 75 km NNE of the tree-ring sampling locations in the Khangai Mountains (Figure 1).

Tree-ring sampling in the Mongolian Altai was conducted S and SE of Lake Dayan (48°14'39"-48°16'3" N, 88°50'17"-88°57'0" E) in the Dayan administrative subunit ('bag') in the Altai Tavan Bogd National Park in Bayan-Ulgii Province ('aimag'), western Mongolia, 110 km SW of the city of Ulgii. In the Khangai Mountains, tree-ring sampling was done in the valley of the river Shireegiin Gol (47°29'11"− 47°30'37" N, 96°59'20"−97°13'59" E), about 30 km SSE of the city of Uliastai and 40 km SW of Mt. Otgontenger in Zavkhan province. Both study areas are located in high mountain regions with an elevation of the
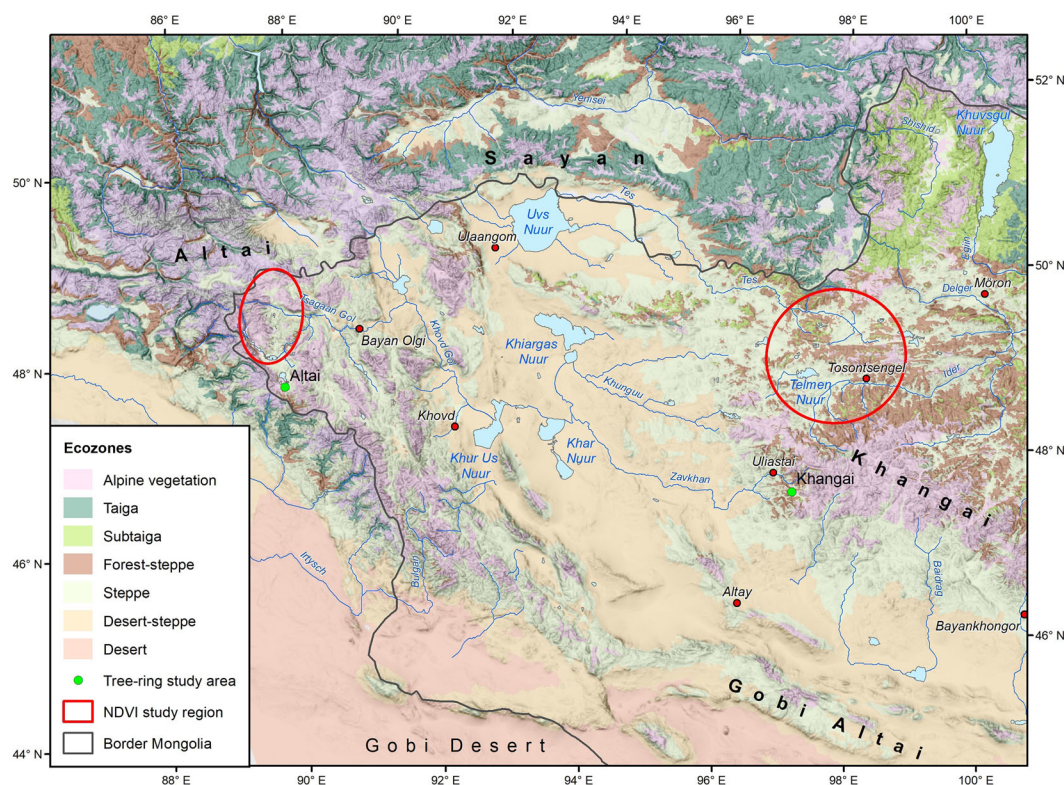
Figure 1. Study areas in the Mongolian Altai and the western Khangai Mountains. Green dots indicate the position of tree-ring sampling sites and red circles represent regions across which NDVI values were averaged.

field sites for tree-ring sampling between ca. 2100 and 2300 m a.s.l. in the Khangai and between about 2300 and 2400 m. a.s.l. in the Mongolian Altai. The mountainous forest-steppe landscapes of the study area are characterized by forests on north-facing slopes and grasslands on south-facing slopes and in dry valleys. All studied forests were monospecific forests of Siberian larch (*Larix sibirica* Ledeb.), a boreal tree species that occupies 75–80% of Mongolia's forest area (Dulamsuren and others 2016). In addition to forests and steppe grasslands, the study area in the Mongolian Altai also included alpine grasslands above the tree line (Figure 1).

Climate

Climate data used in this study were downloaded from https://climexp.knmi.nl using monthly temperature and precipitation data from the CRU TS 4.04 dataset published by the Climate Research Unit of the University of East Anglia, Norwich and the Met Office in Exeter, UK. One-month means of the Standardized Precipitation Evapotranspiration Index (SPEI; Vicente-Serrano and others 2010) were obtained from the same database. All data had a resolution of $0.5° \times 0.5°$ and were downloaded for the periods from 1901 to 2019 (air temperature, precipitation) and 1901 to 2018 (SPEI), except for the Khangai, for which precipitation data were only available since 1937. Data were obtained for the grid fields of 48.0–48.5°N, 88.5–89.0°E for the Mongolian Altai and 47.0–47.5°N, 97.0–97.5°E for the western Khangai. Furthermore, climate data were evaluated for major regions of eastern Inner Asia dominated by varying fractions of true steppe and boreal forest, the latter occurring in forest steppes and partly mountain forests. These regions included the northern part of western Mongolia (47.0–50.0°N, 88.0–100.0°E) dominated by forest steppe and steppe, the northern part of eastern Mongolia with forest steppe, mountain taiga, and true steppe (47.0–50.0°N, 100.0–120.0°E), the eastern center of Inner Mongolia with forest steppe and true steppe (40.0–47.0°N, 115.0–125.0°E), and the northern part of eastern Kazakhstan with true steppe, mountainous forest steppe, and mountain forests (48.0–52.0°N, 72.0–84.0°E). Our study areas in the Mongolian Altai and the western Khangai are part of the 'Western Mongolia' region in the climate analysis.

The climate of western Mongolia is highly continental with low winter temperatures and a relatively narrow precipitation peak in summer. The strong concentration of most of the annual precipitation to the summer months is caused by the stable Siberian Anticyclone, which is usually centered over Lake Baikal and prevents the inflow of moist air masses from autumn to spring (Sahsamanoglou and others 1991). Mean annual and July temperatures are lower in the more elevated Mongolian Altai ($- 6.4 \pm 0.1$, $10.6 \pm 0.1°C$) than in the western Khangai ($- 5.7 \pm 0.1$, $11.7 \pm 0.1°C$), whereas January temperatures do not differ (Altai: $- 25.5 \pm 0.3°C$, Khangai: $- 25.2 \pm 0.2°C$). The climate in the whole of western Mongolia is warmer in summer (July: $14.1 \pm 0.1°C$) and in terms of the annual mean ($- 4.6 \pm 0.1°C$), but colder in winter (January: $- 26.8 \pm 0.2°C$), as this region also includes the Great Lake Depression between the Altai and the Khangai, which is lower and partly semidesert. Mean annual precipitation is 262 ± 4 mm (Altai), 235 ± 5 mm (Khangai), and 233 ± 3 mm (western Mongolia). Roughly 20–25% of the annual precipitation is received in July, the month with the highest precipitation. By contrast, January precipitation is very low at 5 mm or less.

Tree-Ring Data

Tree-ring series of *L. sibirica* trees from the Mongolian Altai and the western Khangai Mountains were obtained from wood cores collected in 2010 (Altai) and 2011 (Khangai) from six north-facing mountain slopes in each of these two regions. The sampling design for the selection of forest sites used the natural setting in Mongolia's forest steppe that forest stands occur as more or less isolated patches on the north-facing mountain slopes, leading to a systematic arrangement of forests in the landscape. We selected a mountain range in either study region, where forested north-facing slopes were rather regularly distributed and selected six stands in a row per region. The distance between stands was 2.2 ± 0.5 km in the Altai and 3.8 ± 0.5 km in the Khangai. Plots of 20×20 m were selected where wood cores of all trees were collected at a height of 1.3 m above the ground, coring parallel of the contour lines of the mountain slope. In each forest, one plot was selected at the forest edge to the grassland (with the lower plot border being identical with the usually abrupt forest line). Another sampling location was selected in the forest interior 50–100 m behind the forest line; at this position, 2 (Khangai) or 3 plots (Altai) were established to increase the sample size. The interior plots of each forest stand were not statistically independent from each other. Tree-ring width was measured with a precision of 10 μm on a movable object table (Lintab 6, Rinntech, Heidelberg, Germany);

TSAP (Time Series Analysis and Presentation)-Win software (Rinntech) was used for measurements and data processing during crossdating, chronology building, and standardization. Standardization was based on dividing tree-ring width by moving averages of the tree-ring series, which preserves much of the high-frequency variation (Cook and others 1990). Tree-ring chronologies were built separately for the study regions (Altai, Khangai) and the habitat (edge, interior). Furthermore, trees were divided into four different age classes based on cambial age at 1.3 m height. These age classes included trees older than 160 years ('very old trees'), 101–160-year-old trees ('old trees'), 61–100-year-old trees ('middle-aged trees'), and trees no more than 60 years ('young trees'). Tree-ring series used for the calculation of mean curves had 'Gleichläufigkeit' (GL) values above 60% ($P \leq 0.05$) and t-values greater than 3; this applied to about 90% of the tree-ring series. This way, several chronologies were built differentiating between regions, habitats, and tree age, and analyzed separately for relationships with the NDVI. These chronologies represent a subset of all chronologies we had available from the study regions (Dulamsuren and others 2014).

NDVI Data

NDVI data used in this study were taken from the Global Inventory Modeling and Mapping Studies (GIMMS) NDVI dataset (NDVI3g; Pinzon and Tucker 2014). The GIMMS NDVI3g product is one of several products that were derived from imagery of the Advanced Very High Resolution Radiometer (AVHRR) sensor series. The GIMMS NDVI3g dataset has been shown to have high temporal consistency compared to other available NDVI datasets and is thus suited for trend analysis (Tian and others 2015). It consists of biweekly maximum value composites of NDVI data at a spatial resolution of 8×8 km^2. The NDVI is calculated as the normalized difference of the spectral reflectance in the red and near infrared region of the electromagnetic spectrum (Tucker 1979). In our study, we used all available data for the period January 1982 to December 2010 and aggregated the biweekly data to monthly maximum value composites. Temporal profiles of NDVI were extracted for the pixels that cover the two regions. Subsequently, the temporal data were averaged in the spatial domain at the level of the two regions (Figure 1). A total of 105 pixels (6720 km^2) in the Altai and 330 pixels (21,120 km^2) in the more spacious landscape structure of the Khangai were included in the

analysis. Due to the spatial resolution of the data, the pixels mostly represent a mixed signal between forest and steppe areas. This also reflects the overall forest-steppe landscape in the two regions.

Reconstruction of Vegetation Greenness

Past vegetation greenness prior to the availability of remote sensing data was reconstructed using tree-ring data. Grouping of the tree-ring series after tree age, habitat, and similarities in growth characteristics (as assessed by GL and t-value) yielded 5 and 16 standardized chronologies from the Mongolian Altai and the western Khangai, respectively, which could be used for the reconstruction of monthly maximum NDVI values. In a first step, a Pearson correlation matrix was calculated for all combinations of tree-ring indices and monthly NDVI values for the period from 1982 to 2010 owing to the availability of remote sensing and dendrochronological data (Tables S1 and S2 in the Supplementary Information). These linear correlations were calculation for both the tree-ring index of the current year and the year after the NDVI observation, as lagged growth responses of stemwood formation are common (Dulamsuren and others 2011, 2013; Wong and others 2021). We selected the most significant linear model with the highest Pearson correlation coefficient (r) and the lowest P value per month (NDVI data) and study region to model the NDVI by ordinary least squares regression. Regression models with $|r| < 0.35$ were generally excluded from further analysis. The goodness of the fit of the modeling results was assessed by calculating r and P values, root mean square errors (RSME) and checking for homoscedasticity. The resulting regression equations were used to reconstruct the monthly maximum NDVI series backward to 1940 (in the case of the Mongolian Altai the selected tree-ring chronology started in 1941). A longer reconstruction was not intended as the estimation error is increasing with the length of the reconstructed time series and because the extension of the NDVI series by four decades was sufficient to solve our research question. We refrained from applying a calibration–verification approach in our reconstruction (Fritts and others 1990; Shi and others 2020; Wang and others 2021), because the length of the time series available for reconstruction made it inadvisable to subdivide the data for regression analysis. Although we always used the most significant models from the correlation matrix reaching back to the 1940s for NDVI reconstruction, we also reconstructed the NDVI from models that were almost as significant as the

best model as an additional control (data not shown), obtaining very similar results as with the selected models.

Our objective to reconstruct NDVI data in large areas of grassland-dominated, but mixed vegetation differed from other approaches where vegetation greenness of forested or grassland-dominated areas (Liang and others 2006; Correa-Díaz and others 2019; Erasmi and others 2021) was modeled on small spatial scales in close vicinity of the tree-ring sampling sites. It is obvious that covering larger areas with mixed vegetation reduces the strength of the correlations and thus details of high-frequency variation are less well captured by the model. However, as we were most interested in the long-term trend and Erasmi and others (2021) already established close correlation between *Larix sibirica* tree-ring indices and grassland NDVI (though weaker than with forest NDVI) with data from the Mongolian forest steppe, we accepted the risk of reduced accuracy in the high-frequency variation, as we were interested to obtain information of the long-term trend from a larger area for our research question.

Statistical Analysis

Arithmetic means ± standard errors (SE) are given throughout the paper. Statistical analyses were calculated in R 4.1.3 software (R core team, Vienna, Austria). Pearson correlation matrices for the selection of tree-ring chronologies for NDVI reconstruction were calculated with the R package HMisc 4.7–1. Annual temperature and precipitation data were examined for temporal trends using linear ordinary least squares regression or nonlinear regression fitting the data to an exponential function. Data were tested for normal distribution with the Shapiro–Wilk test and for the lack of autocorrelation of the residuals with the Durbin–Watson test (R package lmtest 0.9–40) and graphically using the acf function in R stats 4.1.3 before applying ordinary least squares regression. Since SPEI data reflect by definition meteorological events that can be characterized by high temporal variability and the occurrence of outliers in extreme wet and dry years, we calculated both ordinary least squares regression and robust Theil–Sen regressions (R package RobustLinearReg 1.2.0) for the analysis of temporal SPEI trends. Moreover, we used empirical cumulative distribution functions (ECDF; calculated in R stats) for SPEI data grouped by decade for the identification of temporal trends. Linear trends in modeled and measured data of NDVI time series were consistently analyzed with

robust Theil–Sen regressions to exclude the potential influence of outliers. RSME was calculated with R package Metrics 0.1.4, as was the Breusch–Pagan test using R package lmtest (with $P > 0.05$ indicating lack of heteroscedasticity). Cubic splines were calculated with Xact 8.03 software (SciLab, Hamburg, Germany).

RESULTS

Climate Trends in Western Mongolia

Temperature entered an exponential growth in the late 1970s/early 1980s (Figure 2). The linear increase in mean annual temperature since 1901 has been 0.18–0.20 K decade^{-1}. Since 1970, temperatures have increased at a rate of 0.38 K decade^{-1} in the Altai, 0.46 K decade^{-1} in the Khangai and 0.42 K decade^{-1} in the entire western Mongolian forest-steppe region. Annual precipitation in the Mongolian Altai has increased gently by 3 mm decade^{-1} since 1901 and 6 mm decade^{-1} since 1970. No trend for precipitation occurred in the western Khangai or throughout western Mongolia.

A significant trend for increasing aridity, quantified by a decrease in the SPEI in the warmest, but also rainiest month July, was observed for western Mongolia from 1970 to 2018 (Figure 3). Similar tendencies for subareas of the Mongolian Altai and the western Khangai within this region were not statistically significant. In contrast to the long-term trend, western Mongolia experienced a sharp and significant increase in SPEI values (indicating wetter conditions) from 1980 to 1998, both for the entire area and when data from the Altai and Khangai were analyzed separately. This was demonstrated by both linear regression (Figure 3a, c, e) and the analysis of empirical cumulative distribution functions (ECDF) where SPEI data were grouped by decade (Figure 3b, d, f). The linear SPEI trends were hardly influenced by outliers, but the result of long-term trends, as becomes evident from the comparison of the results of linear ordinary least squares and robust Theil–Sen regressions, which only showed an outlier effect on the transient increase in moisture in the 1980s and 1990s in the western Khangai (Figure S1).

Trends in Vegetation Greenness

The monthly maximum NDVI began at the same level in March at the end of winter in both the Mongolian Altai and the western Khangai (Figure 4). By April and through September, the NDVI in the Khangai exceeded that of the Altai (reflecting earlier snowmelt at lower elevation and—based
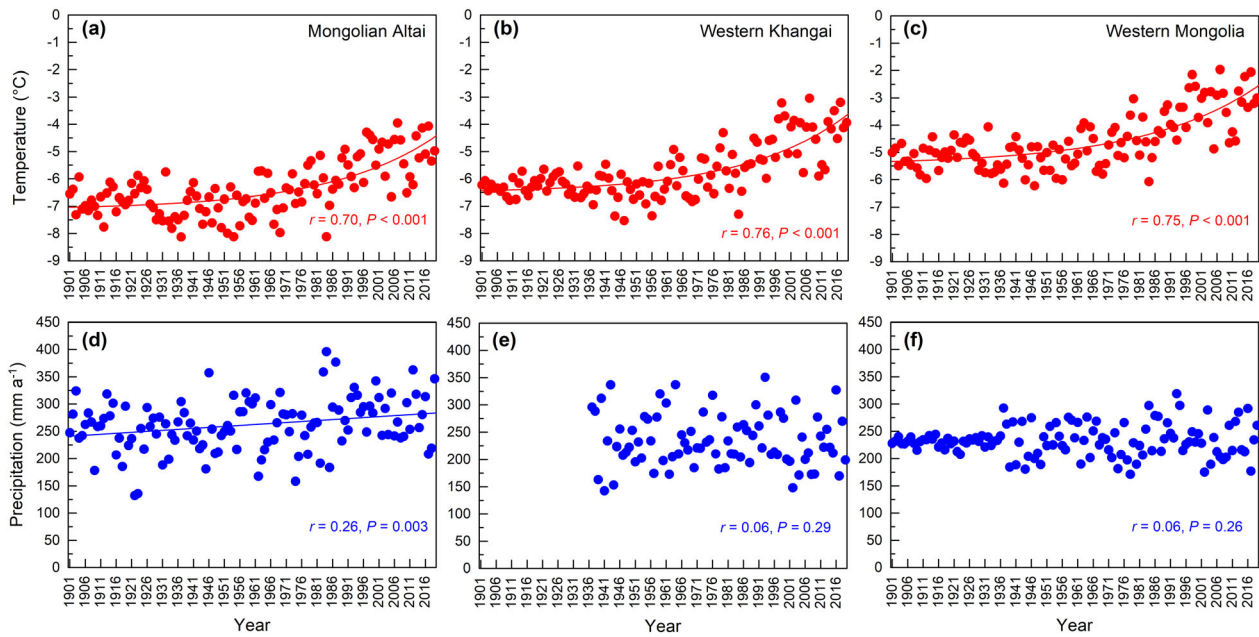
Figure 2. Trends for (**a–c**) mean annual temperature and (**d–f**) annual precipitation for the Mongolian Altai (**a, d**), western Khangai Mountains (**b, e**), and the entire western Mongolian forest-steppe region from 1901 to 2019. Modeled data at a resolution of $0.5° \times 0.5°$ for the grid fields of **a** 48.0–48.5°N, 88.5–89.0°E, **b** 47.0–4/.5°N, 97.0–97.5°E, and **c** 47.0–50.0°N, 88.0–100.0°E (https://climexp.knmi.nl).

on our field observations—taller grassland vegetation in the Khangai). At the end of the growing season in October, the maximum NDVI resumed similar values in both regions.

In the Mongolian Altai, the maximum NDVI showed significant ($P \leq 0.05$) increases between 1982 and 2010 in April, June, and October and a marginally significant ($P \leq 0.10$) trend for increase in May (Figure 4). The March, July, August, and September NDVI remained constant over the years. In the western Khangai, significant increases in the NDVI took place in March, April, and October. Trends for decreasing maximum NDVI were found in June and July, whereas no trends of change occurred in the remaining months (May, August, and September). The temporal trends for monthly maximum NDVI were not influenced by outliers, as the results obtained from robust Theil–Sen regression (Figure 4) were not significantly different from results of ordinary least squares regression (Figure S2).

Peak vegetation greenness was positively correlated with temperature in the Mongolian Altai, but with moisture (that is, precipitation and SPEI) in the western Khangai (Table 1). This became evident from linear regressions between climate variables and means of monthly maximum NDVI calculated for the three summer months (June to

August; Table 1), at a point in time when the NDVI peaked in both study regions (Figure 4).

Reconstruction of the Monthly Maximum NDVI from Tree-Ring Data

Significant linear correlations between standardized tree-ring width and monthly maximum NDVI values were found for spring and early summer and occurred with both tree-ring data of the current and the following year (Tables S1, S2). Reconstructions reaching back to 1940 were obtained for the monthly maximum NDVI of April, May, and June in the Mongolian Altai (Table 2; Figure 5) and of March, April, and June in the less highly elevated western Khangai (Table 2; Figure 6). These relationships were established for a group of middle-aged trees from the Mongolian Altai (Figure S3a) and for old and very old trees from the western Khangai (Figure S3b). Most tree-ring chronologies selected for modeling derived from the forest edge and thus the immediate neighborhood of steppe grasslands (Table 2). All these chronologies had positive growth anomalies in the late 1990s/early 2000s in common (Figure S3). In addition, the tree-ring chronology from the Mongolian Altai exhibited a multi-year growth depression from ca. 1980 to 1995.
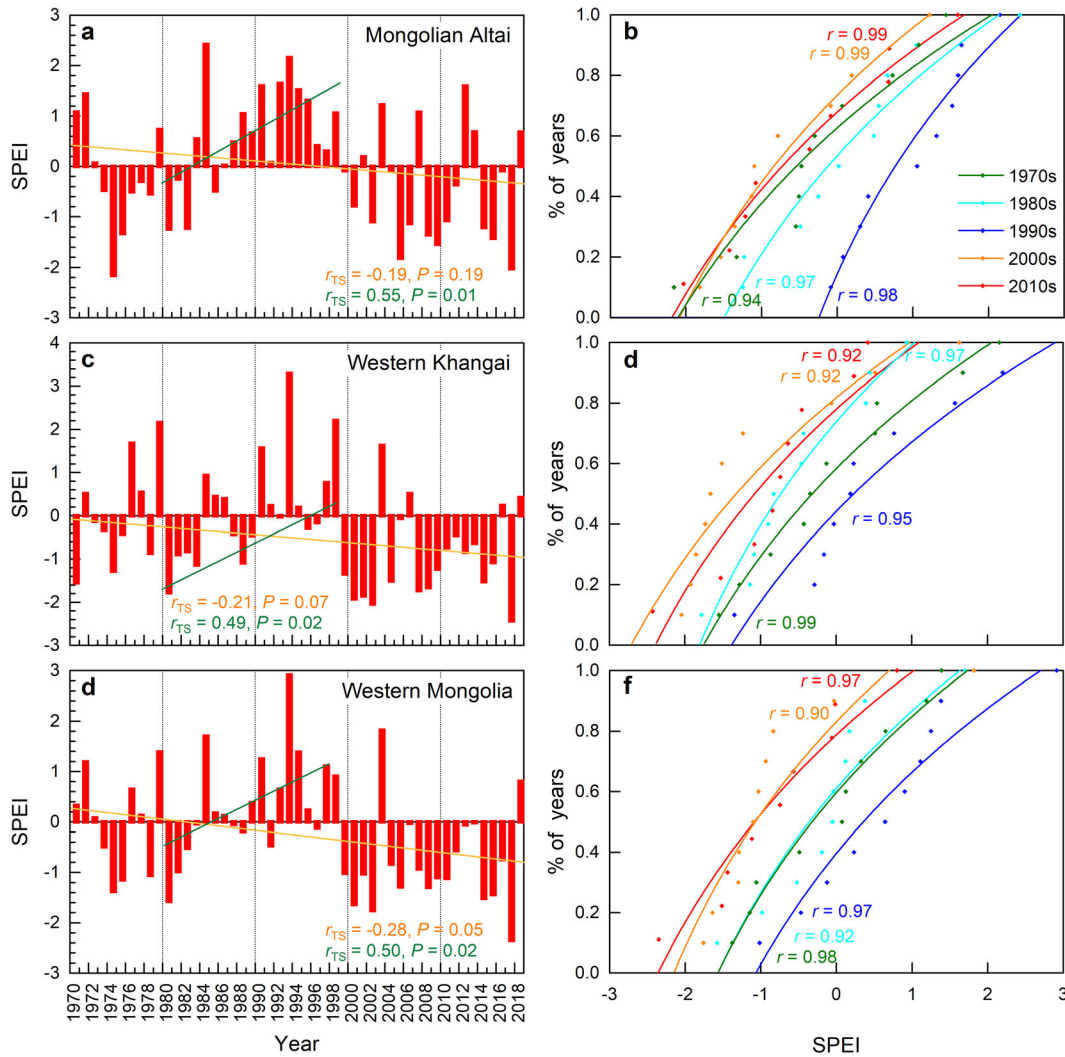
Figure 3. a, **c**, **e** July means and **b**, **d**, **f** empirical cumulative distribution functions (ECDF) of one-month values of the Standardized Precipitation Evapotranspiration Index (SPEI) for 1970–2018 from **a**, **b** the Mongolian Altai, **c**, **d** the western Khangai Mountains, and **e**, **f** the entire western Mongolian forest-steppe region. Modeled data at a resolution of $0.5° \times 0.5°$ for the grid fields of **a** 48.0–48.5°N, 88.5–89.0°E, **c** 47.0–4/.5°N, 97.0–97.5°E, and **e** 47.0–50.0°N, 88.0–100.0°E (https://climexp.knmi.nl). **a**, **c**, **e** Linear Theil–Sen regressions (with Theil–Sen correlation coefficient r_{TS}) for 1970–2018 (orange) and 1982–1998 (green). **b**, **d**, **f** Nonlinear logarithmic regressions of ECDF ($P < 0.001$ for $r > 0.91$; $P < 0.01$ for $r > 0.90$) for SPEI data grouped by decade.

The linear trends for increase in the recorded monthly maximum NDVI from 1982 to 2010 for spring and summer in the Altai and spring in the Khangai (green lines in Figures 5 and 6) corresponded to similar linear relationships in the modeled data (orange lines). Nevertheless, the slopes of the regression lines in the recorded data were generally steeper than those of the modeled data. These differences resulted from the fact that, while the long-term trend and the position of relative maxima and minima of the NDVI along the timeline could be modeled well from the tree-ring data, the amplitude of the high-frequency vari-ability was less well captured. The amplitude of the modeled NDVI series was generally lower than that of the recorded data, resulting in lower residuals, but sometimes even higher correlation coefficients in the linear regressions for the modeled data. In contrast to the Altai (Figure 5c), both the modeled and the instrumental June NDVI exhibited trends for decreasing vegetation greenness after 1982 in the Khangai (Figure 6c).

Long-term trends for the monthly maximum NDVI were modeled since 1940 (Khangai) and 1941 (Altai). In contrast to the predominant in-creases of the modeled and recorded NDVI values
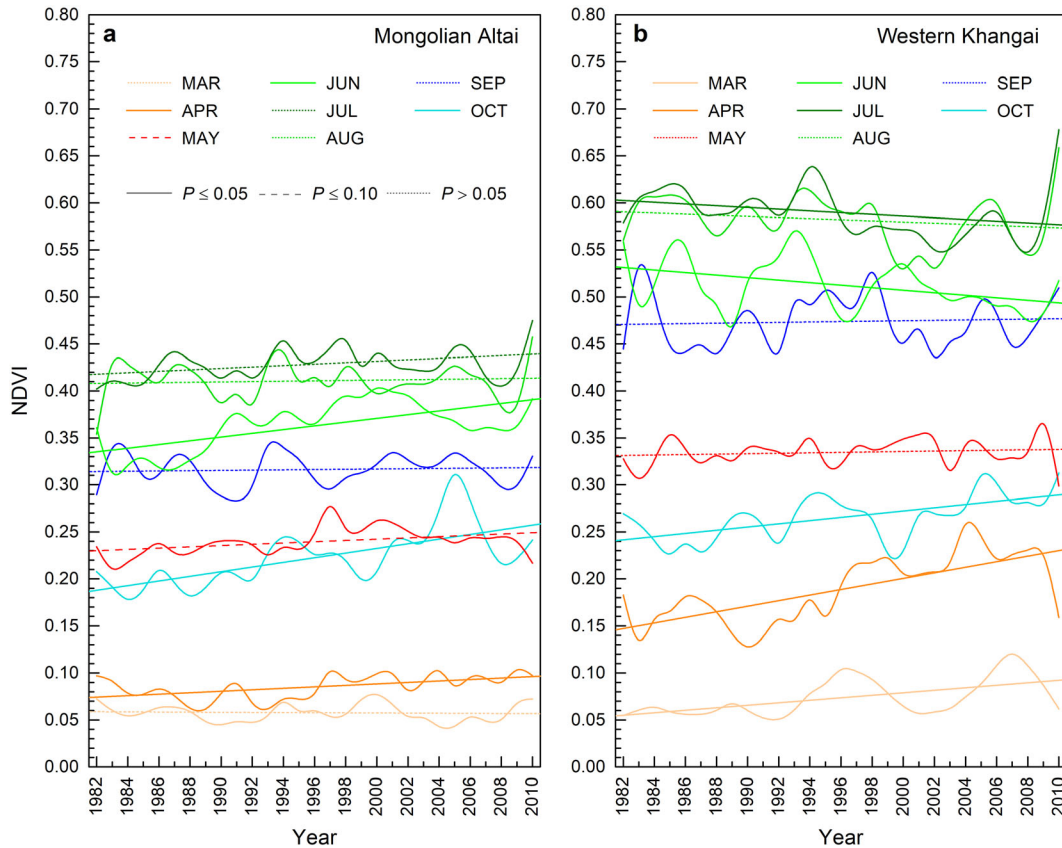
Figure 4. Recorded monthly maxima of the NDVI from 1982 to 2010 (March to October) for **a** the Mongolian Altai and **b** the western Khangai. Cubic spline approximations (with 50% frequency cutoff) and linear Theil–Sen regressions

Table 1. Linear Correlations of Summer NDVI and Climate Variables in the Mongolian Altai and the Western Khangai Mountains

	Mongolian Altai	Khangai
Temperature	0.40/0.02	–0.40/0.02
Precipitation	0.08/0.34	0.65/ < 0.001
SPEI	0.03/0.44	0.58/ < 0.001

Pearson correlation coefficients (r) and P values (r/P). Correlations for the seasonal mean (period June to August) of monthly mean values for air temperature, precipitation, SPEI and maximum NDVI.

after 1982, no long-term NDVI increase could be detected for the period from 1940/41 to 2010 (red lines in Figures 5 and 6). The linear regression lines for the modeled NDVI of this period always showed no significant trend for increase or decrease as estimated with Theil–Sen regression (Figures 5, 6).

SPEI Trends for Eastern Inner Asia

Western Mongolia exhibits similar characteristics of successive dry and wet periods in the early 1980s

and the 1990s as other major steppe and forest-steppe regions in eastern Inner Asia (Figure 7). The July SPEI was negative indicating summer drought during the short period from 1980 to 1982 in western and eastern Mongolia, Inner Mongolia, and eastern Kazakhstan. In all these regions, the period 1990–1999 represented a wet phase as indicated by positive SPEI values. The intensities of both dry and wet phases were highest in western Mongolia and least in eastern Kazakhstan.

Neither in the Mongolian Altai nor the western Khangai, dry and wet phases showed a fixed periodicity during the period from 1901 to 2018, based on July SPEI values (Figure 8). Intervals between drought minima ranged from 6 to 27 years in the Mongolian Altai (Figure 8a) and from 12 to 31 years in the western Khangai (Figure 8b). On a larger geographical scale for all of western Mongolia (Figure 8c), drought minima recurred approximately every 24–28 years in 1922, 1946, 1974, and 2001 over the period from 1901 to 2018. The twenty-first century was, so far, generally dominated by low SPEI values in the western

Table 2. Linear Ordinary Least Squares Regression Equations ($y = a + b$x) Used for Modeling the NDVI From Tree-ring Index Data with Pearson Correlation Coefficients (r), P Values, Root Square Mean Error (RSME), P Value of Breusch–Pagan test (Heteroscedasticity at $P > 0.05$) and Reference to Used Tree-ring Chronology (From Forest Edge, FE or Forest Interior, FI) with Number of Sample Trees (N) and Data Selection for Regression (Tree-ring Index of the Current Year vs. Following Year, 1 Year Lag)

Month	a	b	r	P	RSME	Breusch–Pagan: P	Chronology	N	Data selection
Altai:									
April	0.0601 ± 0.0098	0.0285 ± 0.0105	0.46	0.006	0.847	0.55	AEMM-FE	11	Current year
May	0.2173 ± 0.0109	0.0251 ± 0.0117	0.38	0.02	0.705	0.34	AEMM-FE	11	Current year
June	0.3123 ± 0.0181	0.0573 ± 0.0195	0.49	0.003	0.590	0.43	AEMM-FE	11	Current year
Khangai:									
March	0.1261 ± 0.011	-0.0529 ± 0.010	-0.71	< 0.001	0.973	0.21	OL2-FE	15	1 year lag
April	0.2912 ± 0.031	-0.1060 ± 0.032	-0.55	0.001	0.809	0.50	VO4-FE	15	1 year lag
June	0.4597 ± 0.022	0.0535 ± 0.021	-0.43	0.009	0.558	0.26	H3V-FI	15	Current year

Khangai, entire western Mongolia, and to a lesser extent also in the Mongolia Altai.

DISCUSSION

Potential of Tree-Ring Data for NDVI Reconstruction

Our data show that modeling monthly maximum values of the NDVI from tree-ring data is feasible for the Mongolian forest steppe, where mostly small stands of boreal forest and steppe grasslands alternate in varying proportions. These results add to correlations found between the maximum growing season NDVI and tree-ring anomalies, which were obtained, like the data of the present study, from *L. sibirica* tree-ring data in the Mongolian forest-steppe and Landsat NDVI time series (Erasmi and others 2021). In that study working on a much smaller spatial scale, it was pointed out that the correlation between standardized tree-ring width and the maximum growing season NDVI was stronger for remote sensing data from forested land compared to grasslands, which is obvious as both annual stem increment and forest NDVI are direct measures of forest productivity. By contrast, the relationship to grassland NDVI is weakened by the differences in microclimate between forests and grasslands (Kelliher and others 1993; Dulamsuren and Hauck 2008; Brümmer and others 2012). Moreover, forests and grasslands also differ in their water and carbon relations, as late-successional conifers have a more sensitive stomatal regulation

than grasses, which reduces the mortality risk, but also lowers the carbon gain during dry phases in the former (James and others 2003; Ponton and others 2006).
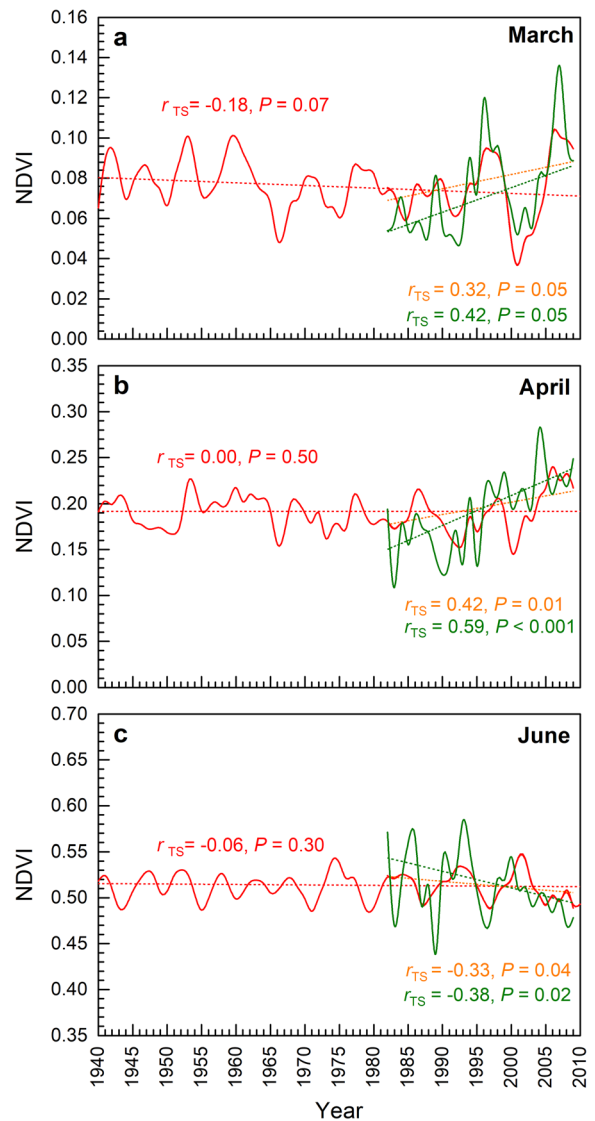
Given the similarities in microclimate between forest edges and grasslands, it is not surprising that Erasmi and others (2021) found close correlations of the maximum growing season NDVI of grasslands with tree-ring width from small forests of less than 0.1 km² size. By contrast, tree-ring chronologies from large forests with a more pronounced forest microclimate exhibited no correlation with grassland NDVI. This finding of Erasmi and others (2021) agrees well with the result of the present study that linear correlations of the monthly maximum NDVI were mostly found with tree-ring data from larch trees growing at the forest edge to the grassland, but rarely with trees from the forest interior. Liang and others (2006) examining correlations of the mean growing season NDVI with tree-ring data in Inner Mongolia speak of relict trees in the woodland-steppe ecotone, which is also suggestive of a situation where trees grew under the influence grassland microclimate. NDVI variations within grasslands can be explained in part by the distribution of permafrost, which is expected to occur downslope of large forest stands (Klinge and others 2021).

Our reconstructions from tree-ring chronologies are capable of modeling linear multi-decadal trends for monthly maxima of the NDVI of forest-steppe landscapes that include both forests and grasslands. The models have their limitations at emulating the
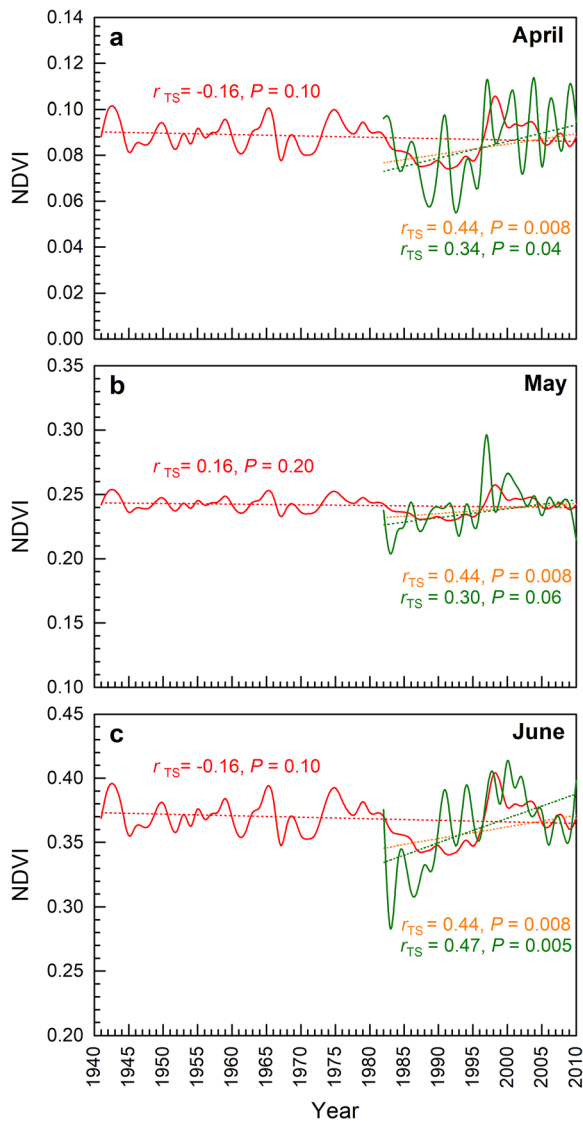
Figure 5. Recorded NDVI (period 1982–2010; green color) and NDVI reconstructed from tree-ring data (1941–2010; red) from the Mongolian Altai for **a** April, **b** May, and **c** June. Cubic spline approximations (with 80% frequency cutoff). Dotted lines represent Theil–Sen robust linear regressions (in red for the complete reconstruction, orange for reconstructed data from 1982 to 2010, and green recorded data from 1982 to 2010).

Fig. 6. Recorded NDVI (period 1982–2010; green color) and NDVI reconstructed from tree-ring data (1940–2010; red) from the Khangai Mountains for **a** March **b** April, and **c** June. Cubic spline approximations (with 80% frequency cutoff). Dotted lines represent Theil–Sen robust linear regressions (in red for the complete reconstruction, orange for reconstructed data from 1982 to 2010, and green recorded data from 1982 to 2010).

amplitudes of interannual NDVI variability. The large areas covered by the remote sensing data in our models (which was necessary for our research question) and the coarse pixel size certainly limited the models' accuracy. In addition, the aforementioned differences in water and carbon relations between forests and grasslands are also a likely explanation for this weakness of our model. Grasslands maintain high transpiration rates even during drought until soil moisture is depleted (Zha

and others 2010). This strategy allows them the maintenance of high carbon assimilation and thus high productivity boosting the NDVI, because the grassland vegetation can efficiently utilize the high solar irradiation, which is characteristic of such weather conditions. Late-successional trees, however, reduce stomatal conductance (Dulamsuren and others 2009) and are consequently less productive lowering positive NDVI extremes. Yet, under prolonged drought conditions, the grasses'
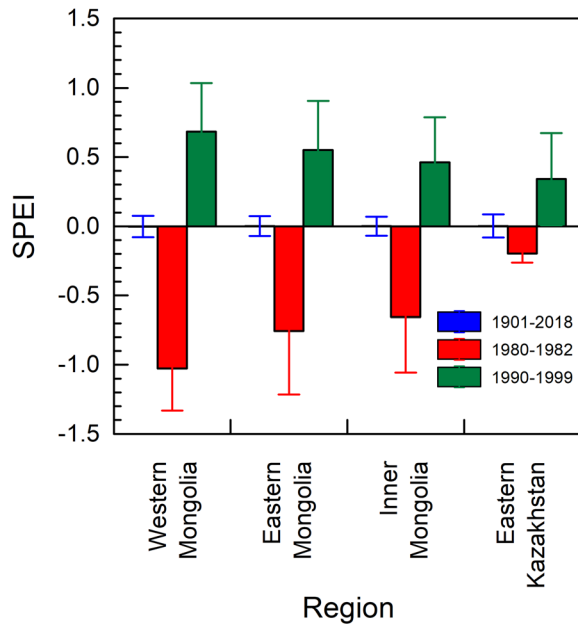
Figure 7. July means (± SE) of one-month values of the Standardized Precipitation Evapotranspiration Index (SPEI) for the periods 1901–2018, 1980–1982, and 1990–1999 from western Mongolian (mainly forest steppe; 47–50°N, 88–100°E), eastern Mongolia (including forest steppe, mountain taiga, true steppe; 47–50°N, 100–120°E), Inner Mongolia (forest steppe, true steppe; 40–47°N, 115–125°E), and eastern Kazakhstan (true steppe, mountainous forest steppe, mountain forests; 48–52°N, 72–84°E). Modeled data at a resolution of 0.5° × 0.5° (https://climexp.knmi.nl).

aboveground parts increasingly yellow and die, thereby reducing the NDVI. Larches and other late-successional conifers, however, usually maintain a green canopy during drought, which protects forests from NDVI declines in a similar range to that in grasslands. These differences between forests and grassland certainly interfere with modeling the amplitude of the interannual variability of the maximum NDVI values for grasslands from tree-ring data, but do not confound multi-decadal trends, because both the maximum NDVI of forests and grasslands in the forest steppes of Inner Asia is primarily controlled by climate (and by moisture in particular) (Prospatin and others 2008; Meng and others 2020).

In the Mongolian Altai, positive tree-ring anomalies were associated with high NDVI values. Since annual stem increment in this region is known to be limited by low summer temperatures (Dulamsuren and others 2014), this result suggests that the grasslands were limited by the same factor. Low temperatures in such high mountain environments are known to be generally limiting for
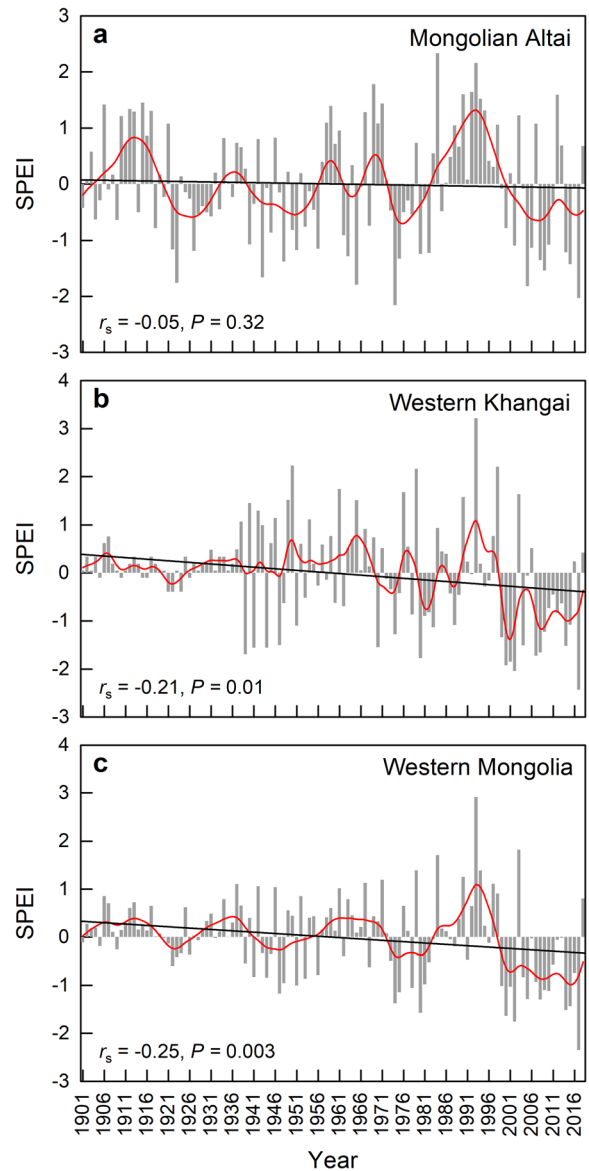
Figure 8. July means of one-month values of the Standardized Precipitation Evapotranspiration Index (SPEI) for 1901–2018 from **a** the Mongolian Altai, **b** the western Khangai Mountains, and the entire western Mongolian forest-steppe region. Modeled data at a resolution of 0.5° × 0.5° for the grid fields of **a** 48.0–48.5°N, 88.5–89.0°E, **b** 47.0–4/.5°N, 97.0–97.5°E, and **c** 47.0–50.0°N, 88.0–100.0°E (https://climexp.knmi.nl). Cubic spline approximations (with 20% frequency cutoff; red lines) and Theil–Sen robust linear regressions (black lines).

vegetation productivity (Xu and others 2016), affecting it both directly and indirectly through low nitrogen availability and by controlling the duration of the snow-free season (Rixen and others 2008; Smith and others 2012). In contrast to our results, Poulter and others (2013) found drought-

limited net primary production on the landscape level, modeled from FPAR, in a region with temperature-limited *L. sibirica* forests in western Mongolia. In the western Khangai, tree-ring anomalies and NDVI values were negatively correlated, while negative correlations of the NDVI with summer temperature and positive correlations with precipitation and SPEI pointed to a drought-limited vegetation greenness productivity on the landscape level, consistent with the widespread drought limitation of larch forests from the Khangai Mountains (Dulamsuren and others 2010a; Poulter and others 2013; Khansaritoreh and others 2017a, 2017b). Drought limitation is typical of steppe grasslands either alone or in combination with temperature and nitrogen limitation (Knapp and others 2001; Guo and others 2014; Li and others 2020; Miao and others 2021). The simultaneous drought limitation of forests and grasslands in the Khangai raises the question why the slopes of the regressions modeling the March and April NDVI from standardized tree-ring width were negative (Table 2). This apparent contradiction can be resolved by considering that high springtime NDVI values are significantly influenced by early snowmelt. Early snowmelt, in turn, increases the risk of drought stress later in the growing season in boreal forests (Parida and Buermann 2014) increasing the probability of low annual stem increment. This matches with the negative NDVI trend found for June in the western Khangai, which is consistent with negative trends established for this area in the remote sensing studies of Mohammat and others (2013) and Poulter and others (2013).

Limitations by Biological Differences Between Forests and Grasslands

Modeling grassland greenness with tree-ring data is based on the fact that the vitality of both grasslands and forests is controlled by moisture and temperature (von Fischer and others 2008; Dulamsuren and Hauck 2021). Nevertheless, there are also biological differences between grasses and trees limiting the commonalities and weakening the relationship between tree-ring width and grassland NDVI. An important factor potentially weakening this relationship is that trees may shift their carbon allocation priorities between different organs more than grasses. Although the difference in the transpiration characteristics between late-successional conifers and grasses is fundamental, rooting depth is another factor that affects moisture utilization by plants (Kelliher and others 1993). This certainly exerts an effect on resource utilization of large, old

trees with extensive and deep rooting systems compared to grasses (Kuiper and Coutts 1992; Dodd and others 1998; Zanetti and others 2015). Yet, for younger trees and grassland species, rooting depth is not fundamentally different. In general, many grasses in the steppe biome have deep root systems (Nippert and Holdo 2015; Walter and Breckle 2021) and can efficiently lower plant water potentials to maintain water uptake from drying soils (Knapp 1985). In this respect, steppe grasses are not necessarily inferior to boreal conifers like *Larix sibirica*, which are able to rapidly lower their water potential due to high cell wall rigidity and active osmotic adjustment (Dulamsuren and others 2009). Chenlemuge and others (2013) analyzed the vertical fine root distribution in the forest steppe of the Mongolian Altai and found of *Larix sibirica* and non-tree fine roots up to a depth of 80 cm, although the decline of fine root mass with depth was steeper in grasses and herbs than larch. Thus, the soil depths from which water is used overlaps between young to middle-aged trees and steppe plants. In contrast to North American prairies, Mongolian grasslands are strongly dominated by C_3 grasses (Still and others 2003); hence, differences in the photosynthetic pathway do not attenuate forest–grassland parallels in the response to climate in Mongolia's forest steppe.

Another limitation arises from the different growth phenologies for stemwood and grassland biomass. Most stemwood in boreal forests is formed in the early growing season (Rossi and others 2016), but summed up in an annual parameter as tree-ring width. Grassland aboveground biomass, which is captured with the NDVI, however, is produced throughout the growing season, as long as climatic conditions are favorable. The restriction of stemwood production to spring and early summer explains why we only found significant correlation with monthly grassland NDVI values from March to June, but not later in summer, which limits our conclusions to trends for vegetation greenness in spring and early summer.

The Greening Trend in Western Mongolia as an Artifact of the Observation Period

From 1982 to 2010, we were able to model the widely known linear trend for increasing vegetation greenness from our tree-ring data. In the Mongolian Altai, significant increases in the model maximum NDVI were observed for April to June in agreement with the results of Poulter and others (2013), who found increasing FPAR values (1982–2010) in spring and summer in this region. In the

western Khangai, significant models showed positive NDVI trends since 1982 for March and April, but (confirm the second hypothesis) a negative trend for June, again in line with Poulter and others (2013), because increases in FPAR in the same period were only found in spring, not summer. By this congruence, our plot-based field data corroborate the existence of the post-1982 greening trend that has been documented by satellite data. However, our data do not suggest that this greening trend is part of a long-term trend for increasing vegetation greenness. Rather, the linear increase since the 1980s has its onset in a temporary period of low vegetation greenness in the 1980s, which was followed by a positive anomaly in the 1990s and 2000s.

Looking back over the four decades prior to the 1980s, it becomes evident that neither the depression in vegetation greenness in the 1980s nor the subsequent increase was unprecedented since 1940. In fact, the reconstructed maximum NDVI values showed decadal to multi-decadal positive and negative anomalies, which followed no or only a very weak negative long-term trend between 1940 and 2010. Our interpretation that the post-1982 vegetation greening is not part of a long-term trend is consistent with a decelerated increase or even transient decline in NDVI values in the late 1990s and 2000s across much of Mongolia, Inner Mongolia, and Kazakhstan (Mohammat and others 2013; Zhang and others 2021). Our conclusions support concerns of Pan and others (2018) that calculating linear trends from series of the NDVI or similar indices sometimes does not fully capture the situation and thus can lead to misinterpretation.

The Putative Absence of a Climate Change-Driven Greening Trend in Eastern Inner Asia

The coincidence of the observed vegetation greening in eastern Inner Asia since the early 1980s with the transition of warming trends into the exponential phase around the same time (Figure 2) was suggestive of the occurrence of a climate change-driven greening trend in Inner Asia's steppes and forest steppes as in the Arctic tundra. However, whereas the greening trend in the Arctic persists and was unprecedented (Berner and others 2020), both properties cannot be attributed to the post-1982 vegetation greening in western Mongolia. While we could substantiate this with our NDVI reconstructions for western Mongolia (confirming our first hypothesis), our results even question the existence of a climate change-driven, persistent

greening trend for the entire Inner Asian grassland and forest-steppe regions. We do not have data to answer this question, but similar sequences of drought summers in the early 1980s and subsequent wet phases in the 1990s in important parts of eastern Inner Asia (Figure 8) suggest the absence of a long-term trend might be general. This conclusion agrees with the conclusions by Liang and others (2006) for Inner Mongolia. While these authors suggested a return interval for dry and wet phases of about 17–20 years based on data reaching back to 1850, our data are less robust in this regard, starting in the 1940s and showing no regular periodicity for either the Mongolian Altai or the Khangai. Whether the recurrence of dry and wet phases every 24–28 years for the larger region of western Mongolia reflects a long-term oscillation remains to be scrutinized.

The post-1982 Inner Asian greening trend is a good example of the need to be cautious in attributing current climatic variability and resulting productivity fluctuations or mortality surges in grasslands or savannas to climate change, because these ecosystems can be subject to substantial fluctuations due to decadal or multi-decadal climate oscillations even without the contribution of climate change (Sala and others 1992; Tilman and El Haddi 1992; Fensham and Holman 1999). Nonetheless, climate is warming rapidly, and both interannual and seasonal variability in precipitation is increasing in the Inner Asian steppe region due to climate change (Sloat and others 2018), suggesting that the already inherently high variability in vegetation greenness of Inner Asia's grasslands and forest steppes could increase further.

DATA AVAILABILITY

Data will be available on request from the authors.

Declarations

Conflict of interest   The authors declare no competing interest.

REFERENCES

Anyamba A, Tucker CJ. 2012. Historical perspectives on AVHRR NDVI and vegetation drought monitoring. In: Anderson MC, Verdin JP, Wardlow BD, Eds. Remote sensing of drought. Innovative monitoring approaches. Boca Raton: CRC Press. pp 23–49.

Babst F, Bouriaud O, Poulter B, Trouet V, Girardin MP, Frank DC. 2019. Twentieth century redistribution in climatic drivers of global tree growth. Sci Adv 5:eeat4313.

Beck PSA, Juday GP, Alix C, Barber VA, Winslow SE, Sousa EE, Heiser P, Herriges JD, Goetz SJ. 2011. Changes in forest productivity across Alaska consistent with biome shift. Ecol Lett 14:373–379.

Berner LT, Massey R, Jantz P, Forbes BC, Macias-Fauria M, Myers-Smith I, Kumpula T, Gauthier G, Andreu-Hayles L, Gaglioti BV, Burns P, Zetterberg P, D'Arrigo R, Goetz SJ. 2020. Summer warming explains widespread but not uniform greening in the Arctic tundra biome. Nat Commun 11:4621.

Bjerke JW, Treharne R, Vikhamar-Schuler D, Karlsen SR, Ravolainen V, Bokhorst S, Phoenix GK, Bochenek Z, Tømmervik H. 2017. Understanding the drivers of extensive plant damage in boreal and Arctic ecosystems: insights from field surveys in the aftermath of damage. Sci Total Environ 599–600:1965–1976.

Brehaut L, Danby RK. 2018. Inconsistent relationships between annual tree ring-widths and satellite-measured NDVI in a mountainous subarctic environment. Ecol Indic 91:698–711.

Brümmer C, Black TA, Jassal RS, and others 2012. How climate and vegetation influence evapotranspiration and water use efficiency in Canadian forest, peatland and grassland ecosystems. Agric For Meteorol 153:14–30.

Buermann W, Parida B, Jung M, MacDonald GM, Tucker CJ, Reichstein M. 2014. Recent shift in Eurasian boreal forest greening response may be associated with warmer and drier summers. Geophys Res Lett 41:1995–2002.

Chenlemuge T, Hertel D, Dulamsuren Ch, Khishigjargal M, Leuschner C, Hauck M. 2013. Extremely low fine root biomass in *Larix sibirica* forests at the southern drought limit of the boreal forest. Flora 208:488–496.

Cook ER, Briffa K, Shiyatov SG, Mazepa VS. 1990. Tree-ring standardization and growth-trend estimation. In: Kairiukstis LA, Ed. Cook ER, . Methods of dendrochronology. Applications in the environmental sciences. Dordrecht: Springer. pp 104–122.

Correa-Díaz A, Silva LC, Horwath WR, Gómez-Guerrero A, Vargas-Hernández J, Villanueva-Díaz J, Velázquez-Martínez A, Suárez-Espinoza J. 2019. Linking remote sensing and dendrochronology to quantify climate-induced shifts in high-elevation forests over space and time. J Geophys Res Biogeosci 124:166–183.

D'Arrigo R, Jacoby G, Pederson N, Frank D, Buckley B, Nachin B, Mijiddorj R, Dugarjav Ch. 2001. Mongolian tree-rings, temperature sensitivity and reconstructions of northern hemisphere temperature. Holocene 10:669–672.

Davi NK, Jacoby GC, Curtis AE, Baatarbileg N. 2006. Extension of drought records for Central Asia using tree rings: west-central Mongolia. J Clim 19:288–299.

Davi NK, Jacoby GC, Fang K, Li J, D'Arrigo R, Baatarbileg N, Robinson D. 2010. Reconstructing drought variability for Mongolia based on a large-scale tree ring network: 1520–1993. J Geophys Res 115:D22103.

De Jong R, Verbesselt J, Schaepman ME, de Bruin S. 2012. Trend changes in global greening and browning: contribution of short-term trends to long-term change. Glob Chang Biol 18:642–655.

Dodd MB, Lauenroth WK, Welker JM. 1998. Differential water resource use by herbaceous and woody plant life-forms in a shortgrass steppe community. Oecologia 117:504–512.

Dulamsuren Ch, Hauck M. 2008. Spatial and seasonal variation of climate on steppe slopes of the northern Mongolian mountain taiga. Grassland Sci 54:17–230.

Dulamsuren Ch, Hauck M. 2021. Drought stress mitigation by nitrogen in boreal forests inferred from stable isotopes. Glob Chang Biol 27:5211–5224.

Dulamsuren Ch, Hauck M, Bader M, Osokhjargal D, Oyungerel Sh, Nyambayar S, Runge M, Leuschner C. 2009. Water relations and photosynthetic performance in *Larix sibirica* growing in the forest-steppe ecotone of northern Mongolia. Tree Physiol 29:99–110.

Dulamsuren Ch, Hauck M, Khishigjargal M, Leuschner HH, Leuschner C. 2010a. Diverging climate trends in Mongolian taiga forests influence growth and regeneration of *Larix sibirica*. Oecologia 163:1091–1102.

Dulamsuren Ch, Hauck M, Leuschner C. 2010b. Recent drought stress leads to growth reductions in *Larix sibirica* in the western Khentey, Mongolia. Glob Chang Biol 16:3024–3035.

Dulamsuren Ch, Hauck M, Leuschner HH, Leuschner C. 2011. Climate response of tree-ring width in *Larix sibirica* growing in the drought-stressed forest-steppe ecotone of northern Mongolia. Ann For Sci 68:275–282.

Dulamsuren Ch, Wommelsdorf T, Zhao F, Xue Y, Zhumadilov BZ, Leuschner C, Hauck M. 2013. Increased summer temperatures reduce the growth and regeneration of *Larix sibirica* in southern boreal forests of eastern Kazakhstan. Ecosystems 16:1536–1549.

Dulamsuren Ch, Khishigjargal M, Leuschner C, Hauck M. 2014. Response of tree-ring width to climate warming and selective logging in larch forests of the Mongolian Altai. J Plant Ecol 7:24–38.

Dulamsuren Ch, Klinge M, Degener J, Khishigjargal M, Chenlemuge T, Bat-Enerel B, Yeruult Y, Saindovdon D, Ganbaatar

K, Tsogtbaatar J, Leuschner C, Hauck M. 2016. Carbon pool densities and a first estimate of the total carbon pool in the Mongolian forest-steppe. Glob Chang Biol 22:830–844.

Erasmi S, Klinge M, Dulamsuren Ch, Schneider F, Hauck M. 2021. Modelling the productivity of Siberian larch forests from Landsat NDVI time series in fragmented forest stands of the Mongolian forest-steppe. Environ Monit Assess 193:200.

Fensham RJ, Holman JE. 1999. Temporal and spatial patterns in drought-related tree dieback in Australian savanna. J Appl Ecol 36:1035–1050.

Fritts HC, Guiot J, Gordon GA, Schweingruber F. 1990 Methods of calibration, verification, and reconstruction. In: Cook ER, Kairiukstis (Eds.) Methods of dendrochronology. Applications in the environmental sciences. Dordrecht: Springer. pp 163–217.

Gedalof Z, Berg AA. 2010 Tree ring evidence for limited direct CO_2 fertilization of forests over the 20th century. Glob Biogeochem Cycles 24:GB3027.

Goetz SJ, Bunn AG, Fiske GJ, Houghton RA. 2005. Satellite-observed photosynthetic trends across boreal North America associated with climate and fire disturbance. Proc Natl Acad Sci USA 102:13521–13525.

Guay KC, Beck PS, Berner LT, Goetz SJ, Baccini A, Buermann W. 2014. Vegetation productivity patterns at high northern latitudes: a multi-sensor satellite data assessment. Glob Chang Biol 20:3147–3158.

Guo L, Wu S, Zhao D, Yin Y, Leng G, Zhang Q. 2014. NDVI-based vegetation change in Inner Mongolia from 1982 to 2006 and its relationship to climate at the biome scale. Adv Meteorol 2014:692068.

Hicke JA, Asner GP, Randerson JT, Tucker C, Los S, Birdsey R, Jenkins JC, Field C, Holland E. 2002. Satellite-derived increases in net primary productivity across North America, 1982–1998. Geophys Res Lett 29:1427.

James SE, Pärtel M, Wilson SD, Peltzer DA. 2003. Temporal heterogeneity of soil moisture in grassland and forest. J Ecol 91:234–239.

Jarvis P, Linder S. 2000. Constraints to growth of boreal forests. Nature 405:904–905.

Kelliher FM, Leuning R, Schulze ED. 1993. Evaporation and canopy characteristics of coniferous forests and grasslands. Oecologia 95:153–163.

Khansaritoreh E, Dulamsuren Ch, Klinge M, Ariunbaatar T, Bat-Enerel B, Batsaikhan G, Ganbaatar K, Saindovdon D, Yeruult Y, Tsogtbaatar J, Tuya D, Leuschner C, Hauck M. 2017a. Higher climate warming sensitivity of Siberian larch in small than large forest islands in the fragmented Mongolian forest steppe. Glob Chang Biol 23:3675–3689.

Khansaritoreh E, Eldarov M, Ganbaatar K, Saindovdon D, Leuschner Ch, Hauck M, Dulamsuren Ch. 2017b. Age structure and trends in annual stem increment of *Larix sibirica* in two neighboring Mongolian forest-steppe regions differing in land use history. Trees 31:1973–1986.

Klinge M, Schneider F, Dulamsuren Ch, Arndt K, Bayarsaikhan U, Sauer D. 2021. Interrelations between relief, vegetation, disturbances, and permafrost in the forest-steppe of central Mongolia. Earth Surf Process Landf 46:1766–1782.

Knapp AK. 1985. Effect of fire and drought on the ecophysiology of *Andropogon gerardii* and *Panicum virgatum* in a tallgrass prairie. Ecology 66:1309–1320.

Knapp AK, Briggs JM, Koelliker JK. 2001. Frequency and extent of water limitation to primary production in a mesic temperate grassland. Ecosystems 4:19–28.

Kruger EL, Volin JC. 2006. Reexamining the empirical relation between plant growth and leaf photosynthesis. Funct Plant Biol 33:421–429.

Kuiper LC, Coutts MP. 1992. Spatial disposition and extension of the structural root system of Douglas fir. For Ecol Manag 47:111–125.

Lara MJ, Nitze I, Grosse G, Martin P, McGuire AD. 2018. Reduced arctic tundra productivity linked with landform and climate change interactions. Sci Rep 8:2345.

Li Q, Hou J, Yan P, Xu L, Chen Z, Yang H, He N. 2020. Regional response of grassland productivity to changing environment conditions influenced by limiting factors. Plos One 15:e0240238.

Liang E, Eckstein D, Liu H. 2006. Assessing the recent grassland greening trend in a long-term context based on tree-ring analysis: a case study in North China. Ecol Indic 9:1280–1283.

Liu H, Park Williams A, Allen CD, Guo D, Wu X, Anenkhonov OA, Liang E, Sandanov DV, Yin Y, Qi Z, Badmaeva NK. 2013. Rapid warming accelerates tree growth decline in semi-arid forests of Inner Asia. Glob Chang Biol 19:2500–2510.

Liu Y, Liu S, Sun Y, Li M, An Y, Shi F. 2021. Spatial differentiation of the NPP and NDVI and its influencing factors vary with grassland type on the Qinghai-Tibet Plateau. Environ Monit Assess 193:48.

McMahon SM, Parker GG, Miller DR. 2010. Evidence for a recent increase in forest growth. Proc Natl Acad Sci U s. a. 107:3611–3615.

Meng M, Huang N, Wu M, Pei J, Wang J, Niu Z. 2019. Vegetation change in response to climate factors and human activities on the Mongolian Plateau. PeerJ 7:e7735.

Meng X, Gao X, Li S, Lei J. 2020. Spatial and temporal characteristics of vegetation NDVI changes and the driving forces in Mongolia during 1982–2015. Remote Sens 12:603.

Miao L, Sun Z, Ren Y, Schierhorn F, Müller D. 2021. Grassland greening on the Mongolian Plateau despite higher grazing intensity. Land Degrad Dev 32:792–802.

Mohammat A, Wang X, Xu X, Peng L, Yang Y, Zhang X, Myneni RB, Piao S. 2013. Drought and spring cooling induced recent decrease in vegetation growth in Inner Asia. Agric for Meteorol 178–179:21–30.

Nemani RR, Keeling CD, Hashimoto H, Jolly WM, Piper SC, Tucker CJ, Myneni RB, Running SW. 2003. Climate-driven increases in global terrestrial net primary production from 1982 to 1999. Science 300:1560–1563.

Nippert JB, Holdo RM. 2015. Challenging the maximum rooting depth paradigm in grasslands and savannas. Funct Ecol 29:739–745.

Pan N, Feng X, Fu B, Wang S, Ji F, Pan S. 2018. Increasing global vegetation browning hidden in overall vegetation greening: insights from time-varying trends. Remote Sens Environ 214:59–72.

Parida BR, Buermann W. 2014. Increasing summer drying in North American ecosystems in response to longer nonfrozen periods. Geophys Res Lett 41:5476–5483.

Piao S, Fang J, Zhou L, Guo Q, Henderson M, Ji W, Li Y, Tao S. 2003. Interannual variations of monthly and seasonal normalized difference vegetation index (NDVI) in China from 1982 to 1999. J Geophys Res 108(D14):4401.

Piao S, Mohammat A, Fang J, Cai Q, Feng J. 2006. NDVI-based increase in growth of temperate grasslands and its responses to climate changes in China. Glob Environ Chang 16:340–348.

Piao S, Wang X, Ciais P, Zhu B, Wang T, Liu J. 2011. Changes in satellite-derived vegetation growth trend in temperate and boreal Eurasia from 1982 to 2006. Glob Chang Biol 17:3228–3239.

Piao S, Nan H, Huntingford C, Ciais P, Friedlingstein P, Sitch S, Peng S, Ahlström A, Canadell JG, Cong N, Levis S. 2014. Evidence for a weakening relationship between interannual temperature variability and northern vegetation activity. Nat Commun 5:5018.

Piao S, Yin G, Tan J, Cheng L, Huang M, Li Y, Liu R, Mao J, Myneni RB, Peng S, Poulter B, Shi X, Xiao Z, Zeng N, Zeng Z, Wang Y. 2015. Detection and attribution of vegetation greening trend in China over the last 30 years. Glob Chang Biol 21:1601–1609.

Pinzon J, Tucker C. 2014. A non-stationary 1981–2012 AVHRR NDVI3g time series. Remote Sens 6:6929–6960.

Ponton S, Flanagan LB, Alstad KP, Johnson BG, Morgenstern KA, Kljun N, Black TA, Barr AG. 2006. Comparison of ecosystem water-use efficiency among Douglas-fir forest, aspen forest and grassland using eddy covariance and carbon isotope techniques. Glob Chang Biol 12:294–310.

Poulter B, Pederson N, Liu H, Zhu Z, D'arrigo R, Ciais P, Davi N, Frank D, Leland C, Myneni R, Piao S, Wang T. 2013. Recent trends in Inner Asian forest dynamics to temperature and precipitation indicate high sensitivity to climate change. Agric For Meteorol 178–179:31–45.

Pretzsch H, Biber P, Schütze G, Uhl E, Rötzer T. 2014. Forest stand growth dynamics in Central Europe have accelerated since 1870. Nat Commun 5:4967.

Propastin PA, Kappas M, Muratova NR. 2008. Inter-annual changes in vegetation activities and their relationship to temperature and precipitation in Central Asia from 1982 to 2003. J Environ Inform 12:75–87.

Rixen C, Freppaz M, Stoeckli V, Huovinen C, Huovinen K, Wipf S. 2008. Altered snow density and chemistry change soil nitrogen mineralization and plant growth. Arct Antarct Alp Res 40:568–575.

Rossi S, Anfodillo T, Čufar K, Cuny HE, Deslauriers A, Fonti P, Frank D, Gričar J, Gruber A, Huang JG, Jyske T. 2016. Patterns of xylem phenology in conifers of cold ecosystems at the Northern Hemisphere. Glob Chang Biol 22:3804–3813.

Ruimy A, Saugier B, Dedieu G. 1994. Methodology for the estimation of terrestrial net primary production from remotely sensed data. J Geophys Res 99:5263–5283.

Sahsamanoglou HS, Makrogiannis TJ, Kallimopoulos pp. 1991. Some aspects of the basic characteristics of the Siberian Anticyclone. Int J Climatol 11:827–839.

Sala OE, Lauenroth WK, Parton WJ. 1992. Long-term soil water dynamics in the shortgrass steppe. Ecology 73:1175–1181.

Schloss AL, Kicklighter DW, Kaduk J, Wittenberg U, Intercomparison TP. 1999. Comparing global models of terrestrial net primary productivity (NPP): comparison of NPP to climate and the normalized difference vegetation index (NDVI). Glob Chang Biol 5(Suppl. 1):25–34.

Shi L, Li G, Liu H, Dech JP, Zhou M, Zhao P, Ren Z. 2020. Dendrochronological reconstruction of june drought (PDSI) from 1731–2016 for the western Mongolian Plateau. Atmosphere 11:839.

Sloat LL, Gerber JS, Samberg LH, Smith WK, Herrero M, Ferreira LG, Godde CM, West PC. 2018. Increasing importance of precipitation variability on global livestock grazing lands. Nat Clim Chang 8:214–218.

Smith JG, Sconiers W, Spasosevic MJ, Ashton IW, Suding KN. 2012. Phenological changes in alpine plants in response to increased snowpack, temperature, and nitrogen. Arct Antarct Alp Res 44:135–142.

Still CJ, Berry JA, Collatz GJ, DeFries RS. 2003. Global distribution of C_3 and C_4 vegetation: carbon cycle implications. Glob Biogeochem Cycles 17:1006.

Tei S, Sugimoto A, Yonenobu H, Matsuura Y, Osawa A, Sato H, Fujinuma J, Maximov TC. 2017. Tree-ring analysis and modelling approaches yield contrary response of circumboreal forest productivity to climate change. Glob Chang Biol 23:5179–5188.

Tian F, Fensholt R, Verbesselt J, Grogan K, Horion S, Wang Y. 2015. Evaluating temporal consistency of long-term global NDVI datasets for trend analysis. Remote Sens Environ 163:326–340.

Tilman D, El Haddi A. 1992. Drought and biodiversity in grasslands. Oecologia 89:257–264.

Tucker CJ. 1979. Red and photographic infrared linear combinations for monitoring vegetation. Remote Sens Environ 8:127–150.

Unkelbach J, Dulamsuren Ch, Behling H. 2021. Late Holocene climate and land-use history in the Mongolian Altai Mountains: combined evidence from palynological, macro-charcoal and tree-ring analyses. Trees For People 4:100073.

Vicente-Serrano SM, Beguería S, López-Moreno JI. 2010. A multiscalar drought index sensitive to global warming: the standardized precipitation evapotranspiration index. J Clim 23:1696–1718.

von Fischer JC, Tieszen LL, Schimel DS. 2008. Climate controls on C_3 vs. C_4 productivity in North American grasslands from carbon isotope composition of soil organic matter. Glob Chang Biol 14:1141–1155.

Walter H, Breckle S-W. 2021 Ökologie der Erde. Band 3 Spezielle Ökologie der gemäßigten und arktischen Zonen Euro-Nordasiens. 3. Edit. Schweizerbart: Stuttgart

Wang T, Bao A, Xu W, Yu R, Zhang Q, Jiang L, Nzabarinda V. 2021. Tree-ring based assessments of drought variability during the past 400 years in the Tianshan mountains, arid Central Asia. Ecol Indic 126:107702.

Wang X, Yi S, Wu Q, Yang K, Ding Y. 2016. The role of permafrost and soil water in distribution of alpine grassland and its NDVI dynamics on the Qinghai-Tibetan Plateau. Glob Planet Chang 147:40–53.

Wong CYS, Young DJN, Latimer AM, Buckley TN, Magney TS. 2021. Importance of the legacy effect for assessing spatiotemporal correspondence between interannual tree-ring width and remote sensing products in the Sierra Nevada. Remote Sens Environ 265:112635.

Zanetti C, Vennetier M, Mériaux P, Provansal M. 2015. Plasticity of tree root system structure in contrasting soil materials and environmental conditions. Plant Soil 387:21–35.

Zha T, Barr AG, van der Kamp G, Black TA, McCaughey JH, Flanagan LB. 2010. Interannual variation of evapotranspiration from forest and grassland ecosystems in western Canada in relation to drought. Agric For Meteorol 150:1476–1484.

Zhang H, Zhang X, Shang Y, Kattel G, Miao L. 2021. Continuously vegetation greening over inner Mongolia for the past three decades. Remote Sens 13:2446.

Zhang P, Jeong J-H, Yoon JH, Kim H, Wang SY, Linderholm HW, Fang K, Wu X, Chen D. 2020. Abrupt shift to hotter and drier climate over inner East Asia beyond the tipping point. Science 370:1095–1099.

Zhao X, Tan K, Zhao S, Fang J. 2011. Changing climate affects vegetation growth in the arid region of the northwestern China. J Arid Environ 75:946–952.

Zhou L, Tucker CJ, Kaufmann RK, Slayback D, Shabanov NV, Myneni RB. 2001. Variations in northern vegetation activity from satellite data of vegetation index during 1981 to 1999. J Geophys Res 106:20069–20083.

Zhu Z, Piao S, Myneni RB, Huang M, Zeng Z, Canadell JG, Ciais P, Sitch S, Friedlingstein P, Arneth A, Cao C. 2016. Greening of the earth and its drivers. Nat Clim Chang 6:791–795.